Predictive feedback control: an alternative to proportional–integral–derivative control

L Giovanini
Department of Informatics, Universidad Nacional del Litoral, Ruta nacional 168, Paraje El Pozo (CC 127), Santa Fe, Argentina. email: lgiovanini@fich.unl.edu.ar

The manuscript was received on 13 April 2009 and was accepted after revision for publication on 17 June 2009.

DOI: 10.1243/09596518JSCE790

Abstract: Even though employed widely in industrial practice, the popular proportional–integral–derivative (PID) controller has weaknesses that limit its achievable performance. In this paper, an alternative control scheme that combines the simplicity of the PID controller with the versatility of model predictive control is presented. The result is a controller that combines the time-delay compensation capability of predictive control algorithms, the effectiveness of inferential control schemes for disturbance rejection, and the adaptation capabilities of switching controllers. The robust stability and performance of the controller are analysed. These results are then used to generate two tuning procedures. The design, implementation, and performance of the controller are illustrated via simulations on linear and non-linear systems.

Keywords: SISO controller design, PID control, controller tuning, disturbance rejection, time-delay compensation, non-linear systems

1 INTRODUCTION

Proportional–integral–derivative (PID) controllers have remained as the most commonly used controllers in industrial process control for more than 50 years, despite advances in mathematical control theory [**1**]. The main reason for this is that these controllers have a simple structure that is easily understood by engineers, and under practical conditions, they perform more reliably than more advanced and complex controllers.

Even though versatile, the PID controller has weaknesses that limit its achievable performance especially on dead-time dominant, inverse response, poorly damped, and non-linear processes. Thus, there has been a continuing interest in devising new ways of approaching the PID tuning and design problems [**2**–**12**]. Available alternatives to the PID controller, provide better performances but at the expense of sacrificing simplicity. These alternatives are also more difficult to tune than the simple PID controller and often require considerable expertise in control theory. It is therefore not surprising that interest in the development of alternatives to the PID controller has grown steadily in recent years [**13**–**15**]. This paper proposes an alternative single-input single-output (SISO) regulatory controller, called predictive feedback control (PFC), that takes advantage of modern control technology to overcome the weaknesses of the PID controller without sacrificing simplicity. The PFC controller combines the time-delay compensation capability of predictive control algorithms, the input reconstruction capabilities of inferential control schemes to improve disturbance rejection, and the adaptation capabilities of switching controllers.

The PFC controller employs only one prediction of the process output J time steps ahead to compute the future error, and the control input $u(k)$ is computed by weighting the predicted errors computed in previous samples. Hence, the resulting control action is computed by observing simultaneously the future and past system behaviour. The adaptation capability can be introduced by an online modification of the prediction time J. Through this mechanism, the closed–loop settling time is modified without affecting closed–loop stability. The resulting controller is a generalization of the internal

mode control (IMC) parametrization, where one of the models employed by the controller parametrization is replaced by a predictor.

The paper is organized as follows: the basic formulation of the PFC controller is derived and the relationship with other control algorithms is established in section 2. Closed–loop stability and performance results are presented in section 3. Then, the adaptation mechanism is discussed and robust stability of the resulting closed–loop system is studied in section 4. In section 5 two simple tuning procedures are developed based on the results of previous sections. In section 6 the implementation of PFC to a linear model of a distillation tower and a non-linear isothermal polymerization reactor are presented. The results obtained with the PFC controller are compared with those of PID controllers tuned using various techniques and a predictive controller. Finally, the results are placed in perspective before the conclusions are presented in section 7.

2 PFC

The PFC control scheme consists of the following three components:

(a) process output prediction;
(b) prediction update;
(c) control action computation;

around which the ensuing section is organized.

2.1 Output prediction

Given the local approximation to the process model is assumed to be an *ARMA* model

$$y(k)=\frac{\tilde{B}(z^{-1})}{1+\tilde{A}(z^{-1})}u(k)+\varepsilon(k) \tag{1}$$

where z^{-1} is the unit delay operator, $\varepsilon(k)$ is the non-measurable disturbance and the polynomials $\tilde{A}(z^{-1})$ and $\tilde{B}(z^{-1})$ are written as

$$\tilde{A}(z^{-1})=\sum_{j=1}^{p}\tilde{\alpha}_j z^{-j},\quad \tilde{B}(z^{-1})=\sum_{j=0}^{p}\tilde{\beta}_j z^{-j} \tag{2}$$

There is no loss of generality assuming that the polynomials have the same order p, since trailing coefficients can be zero. The model (1) can be directly obtained from an identification procedure or from a state space observer [**16**, **17**]. Then, the J-step-ahead prediction, based on the information available at time k, is given by [**18**]

$$\hat{y}(k+J,k)=\sum_{j=0}^{J}\tilde{\beta}_{0y}^{j}u(k+J-j)+\sum_{j=1}^{p}\tilde{\beta}_{jy}^{J}u(k-j)+\sum_{j=1}^{p}\tilde{\alpha}_{jy}^{J}y(k-j)+\varepsilon(k+J) \tag{3}$$

where

$$\tilde{\alpha}_{jy}^{J}=\tilde{\alpha}_{j+1}+\sum_{l=1}^{J}\tilde{\alpha}_l\tilde{\alpha}_{jy}^{J-l},\quad \tilde{\beta}_{jy}^{J}=\tilde{\beta}_{j+1}+\sum_{l=1}^{J}\tilde{\alpha}_l\tilde{\beta}_{jy}^{J-l}\quad J\leqslant p \tag{4a}$$

$$\tilde{\alpha}_{jy}^{J}=\sum_{l=1}^{p}\tilde{\alpha}_l\tilde{\alpha}_{j}^{J-l},\quad \tilde{\beta}_{jy}^{J}=\sum_{l=1}^{p}\tilde{\alpha}_l\tilde{\beta}_{jy}^{J-l}\quad J>p \tag{4b}$$

Equation (3) explicitly contains future values of $\varepsilon(k+J)$ which will be considered in the following section.

2.2 Prediction update

A model cannot be expected to represent the true process dynamics perfectly; but the typical modelling error obtained from available plant measurements ($\varepsilon(k)=y(k)-\hat{y}(k)$) as

$$\varepsilon(k)=\Delta A(z^{-1})y(k)+\Delta B(z^{-1})u(k)+\Delta_S(k)+\delta(k)+w(k) \tag{5}$$

is a combination of several components:

(a) parametric uncertainty $\Delta A(z^{-1})$ and $\Delta B(z^{-1})$ arising from an inaccurate estimation of model parameters;
(b) structural uncertainty $\Delta_S(k)$ arising from the exclusion of higher order, non-linear, process dynamics from the model;
(c) unmodelled disturbance $\delta(k)$ is excluded from the model because it is unmeasurable;
(d) random measurement noise $w(k)$.

The model error $\varepsilon(k)$ can be decomposed into two components that should not be lumped together.

1. The stochastic component of the model error, $\varepsilon_S(k)$, which represents the observable effect of the non-biasing residual features of inherent model uncertainties. It can be characterized by a

zero-mean value, whose statistical moments are indicative of the model's intrinsic integrity and it should not be used to update the model prediction.

2. The deterministic component of the model error, $\varepsilon_D(k)$, which represents the effect of all bias-inducing features. It is the portion of the model error $\varepsilon(k)$ that must be used to update the model prediction to avoid permanent bias.

This idea leads to an update strategy in which $\varepsilon_D(k)$ is estimated from the available model error $\varepsilon(k)$ such that the expected value of the complementary component, $\varepsilon_S(k)$, is required to be exactly zero. From here, the model prediction update strategy consists of two parts:

(a) current disturbance estimation: estimate of the current disturbance effect $\hat{\varepsilon}_D(k, k)$ from $\varepsilon(k)$;
(b) disturbance prediction: predict the future values of the disturbance effect $\hat{\varepsilon}_D(k+J, k)$ using $\hat{\varepsilon}_D(k, k)$.

The current disturbance estimation problem can be solved using an unbiased unknown input observer that reconstructs $\varepsilon_D(k)$ from a known model and known inputs. Such input reconstruction can be achieved through optimal filters that are designed to decouple the residuals from the unknown inputs, generating two groups of residuals: one with zero mean and the others with unknown inputs [**19**–**22**]. The resulting filter is an observer whose gains satisfy some geometrical conditions [**23**]. Once the unbiased filter has been developed, the estimation of the deterministic component of the unmeasurable disturbance $\hat{\varepsilon}_D(k, k)$ is given by [**17**]

$$\hat{\varepsilon}_D(k,k) = \sum_{j=1}^{p} \tilde{\beta}_{j\varepsilon} u(k-j) + \sum_{j=0}^{p} \tilde{\alpha}_{j\varepsilon} y(k-j) \tag{6}$$

Then, the disturbance prediction can be accomplished by building a disturbance predictor following a similar procedure to that described in the previous subsection

$$\hat{\varepsilon}_D(k+J,k) = \sum_{j=0}^{J} \tilde{\beta}^{j}_{0\varepsilon} u(k+J-j) + \sum_{j=1}^{p} \tilde{\beta}^{J}_{j\varepsilon} u(k-j) + \sum_{j=1}^{p} \tilde{\alpha}^{J}_{j\varepsilon} y(k-j)$$

where $\tilde{\alpha}^{J}_{j\varepsilon}$ and $\tilde{\beta}^{J}_{j\varepsilon}$ are given by equation (4). Since the value of future control actions are unknown, this prediction is not realizable. To make it realizable a statement about the future behaviour of the input variable must be done. The simplest rule is to assume that all the inputs will not move over the next J-step-ahead horizon, i.e. $u(k+j) = u(k+j-1)$ $j = 1, \ldots, J$, the predicted process output is given by

$$\hat{\varepsilon}_D(k+J,k) = \tilde{a}_{J\varepsilon} u(k) + \sum_{j=1}^{p} \tilde{\beta}^{J}_{j\varepsilon} u(k-j) + \sum_{j=1}^{p} \tilde{\alpha}^{J}_{j\varepsilon} y(k-j) \tag{7}$$

where $\tilde{a}_{J\varepsilon} = \sum_{j=0}^{J} \tilde{\beta}^{j}_{0\varepsilon}$. Finally, the updated J-step-ahead prediction $\hat{y}(k+J, k)$ is given

$$\hat{y}(k+J,k) = \tilde{a}_J u(k) + \mathcal{P}_u\left(J, z^{-1}\right) u(k) + \mathcal{P}_y\left(J, z^{-1}\right) y(k) \tag{8}$$

where the predictors are given by

$$\mathcal{P}_y\left(J, z^{-1}\right) = \sum_{j=1}^{p} \left(\tilde{\alpha}^{J}_{jy} + \tilde{\alpha}^{J}_{j\varepsilon}\right) z^{-j}$$

$$\mathcal{P}_u\left(J, z^{-1}\right) = \sum_{j=1}^{p} \left(\tilde{\beta}^{J}_{jy} + \tilde{\beta}^{J}_{j\varepsilon}\right) z^{-j}$$

$$\tilde{a}_J = \tilde{a}_{Jy} + \tilde{a}_{J\varepsilon} \tag{9}$$

Remark 1

The prediction (8) includes the future effects of bias-inducing components of the unmeasurable disturbance, introducing an inferential action in the control algorithms to be developed that improves their performance.

Remark 2

If the process includes a measurable disturbance $d(k)$ such that

$$y(k) = \frac{\tilde{B}\left(z^{-1}\right)}{1+\tilde{A}\left(z^{-1}\right)} u(k) + \frac{\tilde{C}\left(z^{-1}\right)}{1+\tilde{A}\left(z^{-1}\right)} d(k) + \varepsilon(k) \tag{10}$$

with $\tilde{C}(z^{-1}) = \sum_{j=0}^{p} \tilde{\gamma}_j z^{-j}$, the disturbance $d(k)$ can be incorporated into $\hat{y}(k+J, k)$, leading to the following expression for the updated prediction

$$\hat{y}(k+J,k) = \tilde{a}_J u(k) + \mathcal{P}_y\left(J, z^{-1}\right) y(k) + \mathcal{P}_u\left(J, z^{-1}\right) u(k) + \left(\tilde{a}_{Jd} + \mathcal{P}_d\left(J, z^{-1}\right)\right) d(k) \tag{11}$$

where $\mathcal{P}_d(J, z^{-1})$ is given by equation (9). In this case, the controller developed with this prediction will include a feedforward action in its structure.

2.3 Control action computation

Once the output prediction has been updated, a single control input move $u(k)$ is computed by minimizing a weighted combination of predicted errors and control actions over a finite horizon [**18**]

$$L(k) = \frac{1}{2}\left[W(z^{-1})\left(\hat{e}^0(k+J,k)-\tilde{a}_J u(k)\right)^2 + R(z^{-1})u^2(k)\right] \tag{12}$$

where $W(z^{-1})$ and $R(z^{-1})$ are stable weighting functions that shape the time domain response. Note that the setpoint signal $r(k)$ can be replaced by a filtered signal $r^*(k) = F_R(z^{-1})r(k)$ such that a new tuning parameter, which shapes the system output for setpoint tracking, can be introduced. Then the control input is given by

$$u(k) = \frac{1}{\tilde{a}_J}\frac{\Theta(z^{-1})}{\Phi(z^{-1})}\hat{e}^0(k+J,k) = F(z^{-1})\hat{e}^0(k+J,k) \tag{13}$$

where the conditional predicted error –the performance deviation that results from $u(k) = 0$– is given by

$$\hat{e}^0(k+J,k) = r(k+J) - \mathcal{P}_y(J,z^{-1})y(k) - \mathcal{P}_u(J,z^{-1})u(k) - \left(\tilde{a}_{Jd} + \mathcal{P}_d(J,z^{-1})\right)d(k) \tag{14}$$

and the polynomials $\Theta(z^{-1})$ and $\Phi(z^{-1})$ are given by

$$\Theta(z^{-1}) = \sum_{j=0}^{w}\theta_j z^{-j} \quad v \geqslant w$$
$$\Phi(z^{-1}) = 1 + \sum_{j=1}^{v}\phi_j z^{-j} \tag{15}$$

The conditional predicted error $\hat{e}^0(k+J, k)$ includes information of two sample times:

(a) the first time index, called prediction time, indicates the number of samples ahead that the system behaviour is predicted (J);

(b) the second time index, called computing time, indicates the time when the prediction is computed.

In this work the delay operator z^{-1} of the compensator $F(z^{-1})$ is applied to the computing time such that

$$u(k) = \sum_{j=0}^{w}\theta_j\hat{e}^0(k-j+J, k-j) - \sum_{j=1}^{v}\phi_j u(k-j) \tag{16}$$

where $\hat{e}^0(k-j+J,\ k-j)$ is the J–step-ahead conditional predicted error based on measurement at time $k-j$.

Thus, with the analytic expression in equation (16), the PFC controller computes, at each time instant k, the control action required to minimize the deviation of the predicted process output from the desired trajectory J steps ahead from the current time instant after the output prediction has been updated to reflect the effect of plant/model mismatch, and conditioned on the fact that only the last w output predictions are used. In other words, given all the input changes, until the instant k, the controller observes the value that would be reached by the system output, if no future control action is taken and then $u(k)$ is computed such that the performance index is minimized.

Remark 3

The weights $W(z^{-1})$ and $R(z^{-1})$ can be selected independently of the system model structure. In this way, the structure of the compensator $F(z^{-1})$ is not connected with the structure of the system model such that $F(z^{-1})$ can be a PI or PID controller while the predictor is built using a high-order or even nonlinear model.

The PFC controller can be derived from the last equation replacing the predicted error (14) with the components in equation (16), the result is

$$u(z) = \frac{\Theta(z)z^J}{\tilde{a}_J\Phi(z) + \Theta(z)\mathcal{P}_u(J,z)}r(z) - \frac{\Theta(z)\mathcal{P}_y(J,z)}{\tilde{a}_J\Phi(z) + \Theta(z)\mathcal{P}_u(J,z)}y(z) - \frac{\Theta(z)(\tilde{a}_{Jd} + \mathcal{P}_d(J,z))}{\tilde{a}_J\Phi(z) + \Theta(z)\mathcal{P}_u(J,z)}d(z) \tag{17}$$

where the first and third terms correspond to the feedforward components of $u(k)$ due to the reference signal $r(k)$ and the measurable disturbance $d(k)$

respectively, while the second term corresponds to the feedback component due to $y(k)$. The resulting controller has a similar structure to a two-degree-of-freedom controller plus a feedforward action, but only three set of parameters to tune: the parameters of polynomials $\Theta(z)$ and $\Phi(z)$ (υ, w, θ_j, and ϕ_j) and the prediction time J. This structure can be extended to a true two-degree-of-freedom structure by prefiltering the signals r and d such that the required degrees of freedom are introduced to shape the system response.

2.4 Relationship with other Control Algorithms

The PFC controller structure consists of a filter $F(z)$ with the J-step-ahead open-loop predictor

$$P(J,z)=\mathcal{P}_u(J,z)+\mathcal{P}_y(J,z)\tilde{G}p(z) \tag{18}$$

and the system model $\tilde{G}p(z)$ in the feedback path (see Fig. 1)

$$C(z)=\frac{F(z)}{1+F(z)\big(P(J,z)-\tilde{G}p(z)\big)} \tag{19}$$

From this equation (and Fig. 1) we can see that the structure of the PFC controller is similar to the IMC parametrization [**24**]. The only difference is the presence of the predictor $P(J, z)$ instead of the model. After some algebraic manipulations the PFC controller $C(z)$ can be rewritten as follows

$$C(z)=\frac{Q(z)}{1-Q(z)\tilde{G}p(z)}$$

where $Q(z)$ is the open–loop controller given by

$$Q(z)=\frac{F(z)}{1+F(z)P(J,z)}$$

Then, the structure of the PFC controller includes the open–loop controller $Q(z)$ with the open–loop predictor in the feedback path. Depending on the value of the prediction time J and the parameters of $F(z)$ different controllers that have been studied in the literature emerge.

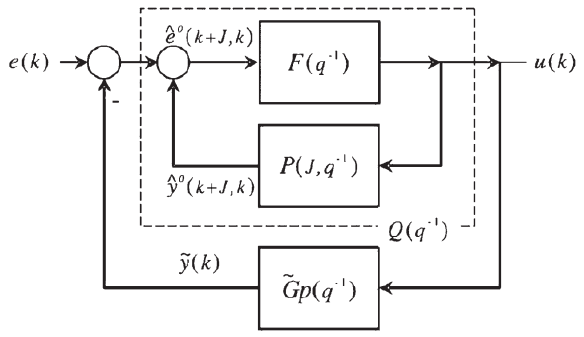

Fig. 1 Structure of the predictive feedback controller [11]

Remark 4

Given the structure of the PFC controller (see Fig. 1 and equation (19)), the compensator $F(z)$ can be designed independently of the predictor $P(J, z)$. Therefore, the structure of $F(z)$ can be fixed independently of the system model $\tilde{G}p(z)$ and its parameters can be determine using a performance index different from equation (12) (see Examples 2 and 3 in this work and examples in [**17**] and [**25**]). In this way, $F(z)$ can have a PID structure while the model is non-linear

For any $J\geqslant\lceil t_d/t_S\rceil$ different controllers are obtained. For the case of $Jt_S=t_d$, the predictor $P(J, z)$ turns into the system model $\tilde{G}p(z)$ without time delay and the PFC controller becomes the Smith predictor [**26**].

When $Jt_S>t_d$ and the parameters of the filter are $w=1,\phi_1=-1,\upsilon=0,\gamma_0=\tilde{a}_J^{-1}$, the resulting controller is the extended horizon controller [**27**]

$$C(z)=\frac{1}{\tilde{a}_J+P(J,z)-\tilde{G}p(z)} \tag{20}$$

which is a generalization of the minimum variance controller. For the particular choice of the prediction time $J=N$, where Nt_S is the open–loop settling time, a family of predictive controllers can be derived. Its main characteristic is to obtain a closed–loop response that is at least as good as the normalized open–loop response. If no other design condition is demanded, the controller (20) becomes the predictor controller [**28**]

$$C(z)=\frac{1}{\tilde{a}_N-\tilde{G}p(z)}. \tag{21}$$

Fixing the parameter of the controller $\gamma_0=\kappa$ $\kappa\geqslant 1$, the simplified model predictive controller [**29**]

$$C(z)=\frac{1}{\kappa^{-1}\tilde{a}_N-\tilde{G}p(z)} \tag{22}$$

is obtained. The parameter κ provides a way to modify the closed–loop response and build dead–time compensation into the controller, but it does not provide offset-free responses in the presence of modelling errors.

From the previous paragraphs it is clear that the PFC controller is a general structure that includes a wide family of controllers, ranging from the classical feedback controller to predictive controllers. It advantage relies on the inclusion of the prediction time J as an additional tuning parameter and the use of past conditional predicted errors ($\hat{e}^0(k-j+J, k-j)$ $j = 0, 1, \ldots, w$) to compute the control action.

3 STABILITY AND PERFORMANCE ANALYSIS

3.1 Stability Analysis

In the first stage a criteria for robust stability under *parametric uncertainty* is derived. Later, the stability criteria will be extended to *polytopic representations* since a family of linear models can approximate a non-linear system with a bounded error [**30**].

Assumption 1

In the following section it is assumed that the unmeasurable disturbance term $\varepsilon(k)$ only includes parametric uncertainty ($\Delta_S(k) = 0$, $\delta(k) = 0$)

$$\varepsilon(k) \simeq \Delta A(z^{-1})y(k) + \Delta B(z^{-1})u(k) \tag{23}$$

The first step to derive a stability criteria is to write the characteristic closed–loop equation $T(J, z)$ in term of the controller parameters, leading to

$$T(J,z) = (1+A(z))\{\tilde{\boldsymbol{a}}_J\Phi(z) + \Theta(z)\mathcal{P}_u(J,z)\} + B(z)\Theta(z)\mathcal{P}_y(J,z) \tag{24}$$

Replacing the predictors $\mathcal{P}_u(J,z)$ and $\mathcal{P}_y(J,z)$ by their components, under Assumption 1, the characteristic equation $T(J, z)$ can be written in terms of the model and controller parameters

$$\begin{aligned} T(J,z) &= \left\{\tilde{\boldsymbol{a}}_J\Phi(z) + \Theta(z)\left[\sum_{j=1}^{p}\tilde{\beta}_j^J z^{-j} + \sum_{j=1}^{p}\left(\beta_j - \tilde{\beta}_j\right)z^{-j}\right]\right\} \\ &\quad \left(1 - \sum_{j=1}^{p}\alpha_j z^{-j}\right) \\ &\quad + \sum_{j=1}^{p}\beta_j z^{-j}\Theta(z)\left[\sum_{j=1}^{p}\tilde{\alpha}_j^J z^{-j} + \sum_{j=1}^{p}\left(\alpha_j - \tilde{\alpha}_j\right)z^{-j}\right] \end{aligned}$$

where α_j and β_j are the plant parameters. The stability of the closed–loop system depends on both: the prediction time J and the parameters of the compensator $F(z^{-1})$, which must satisfy the following relationship.

Theorem 1

Given a system controlled by a PFC controller, the closed–loop system will be robustly stable if

$$\left(1 + \frac{1 - \sum_{j=1}^{v}\left|\phi_j\right|}{\sum_{j=0}^{w}\left|\theta_j\right|}\right)\tilde{\boldsymbol{a}}_J > \sum_{j=1}^{p}\left|\tilde{\beta}_j^J\right| + |K_P|\sum_{j=1}^{p}\left|\tilde{\alpha}_j^J\right| + \sum_{j=0}^{p}\left|\beta_j - \tilde{\beta}_j\right| + |K_P|\sum_{j=1}^{p}\left|\alpha_j - \tilde{\alpha}_j\right| \tag{25}$$

where K_P is the process gain and $\tilde{a}_J$ is the Jth coefficient of the model's step response.

Proof

See [**18**].

When plant and the model are similar, equation (25) becomes

$$\left(1 + \frac{1 - \sum_{j=1}^{v}\left|\phi_j\right|}{\sum_{j=0}^{w}\left|\theta_j\right|}\right)\tilde{\boldsymbol{a}}_J > \sum_{j=1}^{p}\left|\tilde{\beta}_j^J\right| + |K_P|\sum_{j=1}^{p}\left|\tilde{\alpha}_j^J\right| \tag{26}$$

and the stability region is the unit circle.

Remark 5

If the compensator $F(z)$ includes an integral mode

$$\sum_{j=1}^{v}\left|\phi_j\right| = -1 \tag{27}$$

the stability condition (25) becomes

$$\tilde{\boldsymbol{a}}_J > \sum_{j=1}^{p}\left|\tilde{\beta}_j^J\right| + |K_P|\sum_{j=1}^{p}\left|\tilde{\alpha}_j^J\right| + \sum_{j=1}^{p}\left|\beta_j - \tilde{\beta}_j\right| + |K_P|\sum_{j=1}^{p}\left|\alpha_j - \tilde{\alpha}_j\right| \tag{28}$$

This equation is the stability condition of the extended horizon controller [**27**] and the closed–loop stability only depends on the prediction time J. This suggests that the prediction time J and the parameters of the filter can be independently selected such that both, prediction time and the

filter parameters, independently guarantee the closed–loop stability. This fact means that the prediction time J should be selected using equation (28), and the filter must be tuned as there is no time delay in the system, because the predictor $P(J, z)$ has compensated it [**31**].

Closed–loop stability depends on compensator parameters and prediction time J simultaneously. Once the compensator has been tuned, the closed–loop stability only depends on J, which is not unique and can be used to insensitize the system with respect to the value of the system time delay or uncertainties. The set of stable prediction times $\mathcal{S}_S$ is defined as

$$\mathcal{S}_{STB} = \{\forall\, J \in \mathcal{N} \ \wedge\ J \text{ verify equation (25)}\}$$

For a stable system it is easy to verify that $\mathcal{S}_{STB}$ is non-empty and it is given by the union of a finite number of disjoint subsets. This situation only happens for underdamped systems with big natural frequency ω_n compared with the damping factor ζ ($\zeta < 0.01\omega_n$ and $\omega_n \geqslant 0.1$). For this system the dependency of stability horizon is not uniform. However, for critical and overdamped systems the set $\mathcal{S}_S$ is unique ($n = 1$) and the dependency of the stability with J is uniform as it can be seen in the following example.

Example 1

To analyse the dependency of closed–loop stability with the prediction time let us consider the following transfer function

$$Gp_1(z) = \frac{0.0395z + 0.0094}{z^2 - 0.9578z + 0.0067} \tag{29a}$$

$$Gp_2(z) = \frac{0.1044z + 0.0883}{z^2 - 1.4138z + 0.6065} \tag{29b}$$

$$Gp_3(z) = \frac{0.1129z + 0.1038}{z^2 - 1.5622z + 0.7788} \tag{29c}$$

These models are an overdamped system (Gp_1), a critical damped (Gp_2), and an underdamped system (Gp_3) respectively. A graphical representation of the stability condition (26) can be obtained by plotting in the same figure the step response (a_J) of the system and the right term of the stability condition for a given filter

$$r_J = \frac{1}{1 + \left(1 - \sum_{j=1}^{v} |\phi_j|\right) \Big/ \sum_{j=0}^{w} |\theta_j|} \left(\sum_{j=1}^{p} \left|\beta_j^J\right| + |K_P| \sum_{j=1}^{p} \left|\alpha_j^J\right| \right) \tag{30}$$

then, the stable prediction times are given by those ones that verify the inequality $a_J > r_J$. Without loss of generality, it will be assumed that the controller includes an integral mode, then the closed-loop stability will only depend on the prediction horizon J (see equation (28)).

Figure 2(a) shows a_J and r_J of Gp_1 for different prediction horizons J. From this figure it is easy to see that the dependency of closed–loop stability with prediction time is uniform such that the closed-loop system will be stable for $a_J > 1/2K_P$, then the closed-loop system is stable for $J > 15$.

Figure 2(b) shows the same data for Gp_2. From this figure it can be appreciated that for a critical damped system the dependency of closed–loop stability with the prediction time is still uniform. However, the prediction time required to guarantee the closed–loop stability is smaller, and a_J is bigger, than the one required for an overdamped system ($J > 5$, $a_J > 0.85$).

Finally, Fig. 2(c) shows the same data for Gp_3. The non-uniform dependency of closed–loop stability with prediction time can be seen in this figure . The closed–loop system is unstable for $J < 7$, then the closed–loop system becomes stable for $J \in [7,8]$, then it becomes unstable again for $J \in [9,10,11]$ and finally the closed–loop system becomes stable for $J \geqslant 12$.

The previous results are now extended to more sophisticated uncertainties descriptions, which allow the inclusion of structural uncertainty ($\Delta_S \neq 0$). In practice, it is difficult –almost impossible– to know the true model parameters, therefore control engineers generally assume that a polytopic linear model $\mathcal{W}$ of m linear-time-invariant (LTI) models is capable of describing with a given accuracy ε the system behaviour in a bounded domain. Then, the robust stability problem becomes the problem of finding the controller parameters (J, θ_j, and ϕ_j) such that equation (25) is satisfied for each model of $\mathcal{W}$. Equation (25) becomes

$$\left(1 + \frac{1 - \sum_{j=1}^{v} |\phi_j|}{\sum_{j=0}^{w} |\theta_j|}\right) \tilde{\boldsymbol{a}}_J > \sum_{j=1}^{p} \left|\tilde{\beta}_j^J\right| + \left|\tilde{K}_P\right| \sum_{j=1}^{p} \left|\tilde{\alpha}_j^J\right| + \max_{l \in [1,m]} \left(\sum_{j=0}^{p} \left|\beta_{jl} - \tilde{\beta}_j\right| + \left|K_P^l\right| \sum_{j=1}^{p} \left|\alpha_{jl} - \tilde{\alpha}_j\right| \right) \tag{31}$$

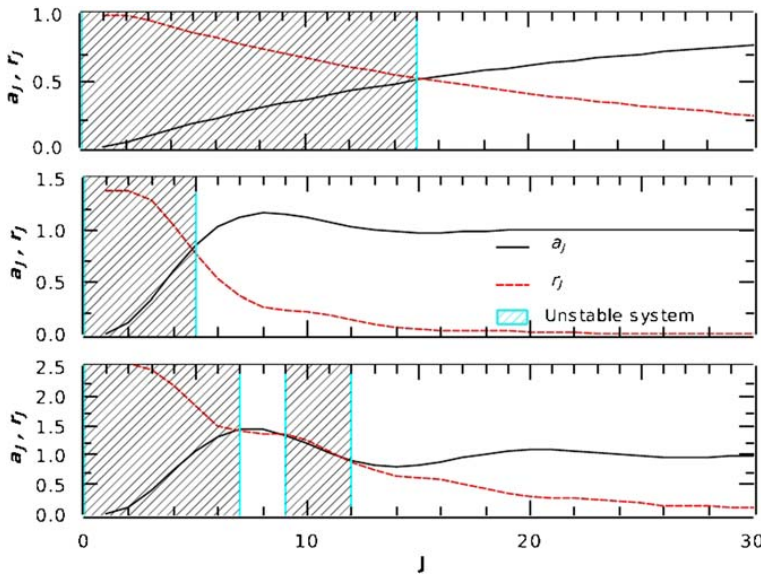

Fig. 2 Dependability of closed–loop stability with the prediction time J for different systems

This condition means that the closed–loop stability for the worst model is guaranteed. From a geometrical point of view, this condition means that the biggest uncertainty $\overline{la} = \max_{l\in[1,m]} la_l$ is employed to determine J, which leads to the smallest robust stability region in order to stabilize the worst model.

The stability criteria derived in this section (equations (25), (26), and (31)) guarantee the superstability of the closed-loop system [**32**], imposing a higher lower bound for selecting the prediction time J than the real one. The conservativeness of this bound depends on the order of the system p, since the poles of a superstable system are confined to an area comprised by all regular polygons with $2k$ sides ($k = 1,\ldots, p,$) inscribed into the unit circle and having one of their vertices at the point +1 [**32**]. Therefore, there are always smaller prediction times than the one provided by stability conditions which leads to a stable closed-loop system. They can be found through a direct search in the set

$$\mathcal{S} = \{\forall\, J \in \mathcal{N} \ \wedge\ J \text{ verify } J_{t_d} \leqslant J\}$$

where $J_{t_d} = \lceil t_d/t_S \rceil$ and Nt_S is the open-loop settling time.

3.2 Performance Analysis

Now, the effects of the PFC parameters on closed–loop performance will be analysed. The PFC control law is given by

$$u(k) = \frac{1}{\tilde{a}_J}\frac{W(z^{-1})}{W(z^{-1}) + \tilde{a}_J^{-2} R(z^{-1})}\hat{e}^0(k+J,k)$$
$$= F(z^{-1})\hat{e}^0(k+J,k)$$

From this equation it can be seen that the weighting functions ($W(z^{-1})$ and $R(z^{-1})$) and the prediction time J determine the closed–loop response features. However, each of these parameters control some distinct characteristics of the closed–loop response.

The weighting functions define the properties of the desired closed–loop response (steady-state error, robustness, overshoot, etc.) by defining the structure and parameters of the compensator $F(z)$. In this way, the weighting functions determine the area where the closed–loop poles will be located. Then, it can be modified by changing the prediction time J, which determines the overall controller gain.

The prediction time J is related to the closed–loop settling time since it defines the time instant of the system output that is controlled, $\hat{y}(k+J, k)$. This fact can be clearly seen if constant weighting functions ($W(z^{-1}) = 1$, $R(z^{-1}) = \rho$) are employed to design the PFC control law.

Theorem 2

The prediction time J is the closed–loop settling time for an error $\lambda e(k)$, $|\lambda| < 1$ and the control weight ρ is related to λ and J through

$$\rho = \frac{\lambda}{1-\lambda}\tilde{a}_J^2 \tag{32}$$

Proof

See [**25**]

When $J = \inf\{\mathcal{S}_{STB}\}$, the controller gain is the largest, the controller drives the system output to

the reference in J steps and the controller becomes the minimum–time control law for the deterministic case or the minimum variance control law for stochastic systems [**28**].

Remark 6

The PFC controller leads to stable closed–loop systems, even for minimum phase systems, because it avoids the cancellation of the unstable portion of the systems by choosing the time when the system output is controlled (the prediction time J). In this way, a kind of spectral factorisation of the system is performed when the prediction time J is chosen and the predictor $P(J, z)$ is built.

If J is increased, the gain of the PFC controller is reduced while the closed–loop settling time is increased. For the particular choice of the prediction time $J = N$ the open–loop settling time, the controller drives the system output to the reference in N time intervals and only one significant control move is observed (minimum–energy control law).

4 ADAPTATION MECHANISM

The predictor $P(J, z)$ is the Youla parameter of the PFC controller (see Section 2.4). If the prediction time J is changed, the open–loop controller $Q(z)$ – and therefore the feedback controller $C(z)$– are modified. In order to guarantee the closed–loop stability $Q(z)$ should be stable, therefore J should be chosen such that it satisfied the stability conditions (equations (25) or (31)).

The online modification of the prediction time J can be employed as an adaptation mechanism to improve the closed–loop performance. In particular, it will be useful when non-linear systems, a linear system with varying time delay and/or significant uncertainties have to be controlled. In this case, assuming that m LTI models represent the system in a bounded domain, different J can be chosen for different operating regions such that similar closed–loop responses are obtained for each region.

It should be pointed out that the proposed adaptation mechanism is related to switching systems due to the nature of the adaptation parameter (J is an integer variable). However, it is different from the classical switching control systems since the Youla parameter (and therefore only the parameters of the controller) of the controller is modified instead of changing the entire controller. In this way, the different controllers that emerge from changing J share their internal states (past measured errors and control actions), avoiding bumps and oscillations due to discontinuities in the control law during the controller switch.

Superstability [**32**] plays a crucial role in the stability analysis of switching systems. It is a necessary and sufficient condition to guarantee the closed–loop stability [**33**]. Discrete superstable systems enjoy numerous important properties, for this work the most relevant are:

(a) superstability guarantees the existence of a positively invariant set;
(b) superstability implies the existence of a non-quadratic Lyapunov function;
(c) superstability is retained in the time-varying case.

Given a system controlled by a PFC controller that changes its prediction time J, the closed–loop stability is guaranteed under the following conditions.

Theorem 3

Given a system controlled by a PFC controller whose prediction time $J(k)$ $\forall k > 0$ and compensator parameters (ϕ_j and θ_j) satisfy the stability conditions (equations (25) or (31)), the resulting closed–loop system is exponentially stable for any bounded reference or disturbance.

Proof

The stability conditions derived in section 3.1 imply the superstability of the closed–loop system. Therefore, if the reference trajectory is bounded ($r(k) \leqslant \mu_R$ $\mu_R > 0$), the closed–loop error trajectories will monotonically decrease for all future samples [**32**]

$$\|e(k)\|_\infty \leqslant \eta(k) + \sigma(k)\max\left(0, \|e(0)\|_\infty - \eta(k)\right), \quad k > 0 \tag{33}$$

where

$$\sigma(k) = \prod_{i=0}^{k} \|T(J(i),1)\|_1, \; \eta(k) = \frac{\|B(1)\Theta(1)\|_1}{1-\sigma(k)} \tag{34}$$

Since the closed–loop error and input trajectory converges monotonically in the norm, the resulting closed–loop system is exponentially stable.

Equation (33) is a non-asymptotic estimates of the closed–loop error $e(k)$, and therefore of the system

output $y(k)$, for arbitrary initial conditions ($|e(k-j| \leqslant \mu_E \ \mu_E > 0, \ j = 1,\ldots,w$). Moreover, super-stable systems are robust with respect to outliers in the inputs [**34**]. Hence, the output of system controlled by a PFC controller will monotonically decrease in the norm until it enters into an invariant set of size $\eta(k)$, where it will remain. Then, it is clear that any change in the prediction time J, that satisfies stability conditions, will not produce chattering in the system output induced by the adaptation mechanism.

5 TUNING PROCEDURES

The PFC controller has several parameters that need to be tuned: the prediction time J and the parameters of the compensator $F(z)$ (order and coefficients of the polynomials $\Theta(z)$ and $\Phi(z)$). From the stability conditions derived in section 3.1 it is easy to see that there is an interaction between the effects of the compensator and the prediction time on closed–loop stability that upsets the tuning procedure. Therefore, the stability conditions induce the following two design procedures.

1. Design procedure 1 (see Fig. 3) starts by fixing the prediction time J, and then finding the compensator $F(z)$ such that robustness and performance requirements are achieved.
2. Design procedure 2 (see Fig. 4) starts by designing the compensator $F(z)$ for the system without time delay and, then the prediction time J is chosen using one of the stability conditions.

When the system is non-linear or linear with changes in the time delay value, one LTI controller can not achieve the system's robustness and performance requirements, then an adaptation mechanism that modifies the controller in a stable way is needed. In this case, design procedure 1 is the more suitable because it takes advantage of the modification of the prediction time: different prediction times can be chosen for different operating regimes, which can be represented by one or several models of a polytope $\mathcal{W}$. Then, the compensator $F(z)$ is designed such that the system's robustness and performance requirements are achieved for each operating regime. During the system operation, the prediction time J will be changed to match the operating regime according to the sequence defined in the design stage.

Design procedure 2 is better for linear systems with moderate or neglected uncertainties and changes of time delay. In this case one LTI controller is enough to achieve the system's robustness and performance requirements. Thus, a prediction time J combined with a properly tuned compensator $F(z)$ are used to implement the PFC controller.

In the following sections these procedures will be employed to develop the controllers in the following examples.

Design Procedure 2

1. Choose the nominal model of the system $\widetilde{G}p(z)$
2. Design the compensator $F(z)$ using $\widetilde{G}p(z)$ without time delay
3. Choose the prediction time J using stability condition (26)
4. Assemble the PFC controller

Fig. 4 Design procedure 2

6 ILLUSTRATIVE EXAMPLES

There are two key characteristics of the PFC controller.

1. Its simplicity: It employs the same process characterization used to design and tune PID controllers; and it computes the control action from an analytical expression that is easy to implement.
2. An improved performance: Because of its predictive formulation, and its systematic approach to disturbance estimation, it delivers improved performance especially for time-delay-dominated processes and for processes with noisy measurements.

Several examples will now be presented to illustrate these characteristics and practical implementation.

Design Procedure 1

1. Choose the nominal model of the system $\widetilde{G}p(z)$ from $\mathcal{W}$
2. Define M $(1 \leq M \leq m)$ operating regimes from $\mathcal{W}$
3. Choose the prediction time for each operating regime $J_l \ l = 1,\ldots,M$ using stability condition (29)
4. Design the compensator $F(z)$ using nominal model, the open-loop predictors for each regime $P_l(J_l, z)$
5. Assemble the PFC controller

Fig. 3 Design procedure 1

Example 2

This example considers a subset of the model of a distillation column provided by Prett and Morari [**35**], whose model is

$$y(s) = 4.05\frac{e^{-27s}}{50s+1}u(s) + 1.44\frac{e^{-27s}}{40s+1}d(s) \tag{35a}$$

$$t(s) = 3.66\frac{e^{-2s}}{9s+1}u(s) + 1.27\frac{1}{6s+1}d(s) \tag{35b}$$

The process has two outputs: the primary output ($y(s)$) that is dominated by the time delay and the secondary output ($t(s)$) responds much faster to manipulated and disturbance variables than $y(s)$.

The controller performance is investigated under disturbance rejection conditions. The control requirements for this problem are: a zero-offset steady-state response and the shortest settling time possible for an error of 0.02. The performance of the PFC controller is compared with that of a cascade scheme, whose controllers were tuned following the IMC design procedure [**36**], and a RTD-A controller [**15**]. To develop the controllers, the model (35) was discretized using a zero-order holder in the input and a sampling time of 1 s. The tuning parameters chosen for the RTD-A controller are: $\theta_R = 0.99$, $\theta_T = 0.1$, $\theta_D = 0.01$, $\theta_A = 0.9$; and the parameters of the controllers for the cascade scheme are: $K_C = 0.81$, $\tau_I = 9$ (inner loop) and $K_C = 0.20$, $\tau_I = 50$, $\tau_D = 10$ (outer loop).

The PFC controller was designed following design procedure 2 using an IMC procedure to design $F(z)$. The predictor for $P(J, z)$ was developed using the entire model of the process, such that the resulting predictor can use the secondary output $t(s)$ to improve the prediction. The predictor was developed from the disturbance estimator built around the space state model of the process, assuming a deadbeat behaviour in the observer. The prediction time J was chosen using the stability condition (28)

$$J \geqslant 38$$

Since this stability condition is conservative, the solution space ($27 \leqslant J \leqslant 38$) is explored and the prediction time that provides the better performance is $J = 28$ (see Fig. 5). The remaining parameters of the PFC controller are: $\nu = 1$, $\phi_1 = -1$, $w = 1$, $\theta_0 = 6.1728$, and $\theta_1 = -5.8642$.

Figure 5 shows the responses of the PFC controller for different values of J. The first thing that can be seen is that the system is stable for smaller values of J than the ones predicted by stability condition (26). This over-design is due to the conservative nature of the stability criterion employed to develop the stability conditions for the PFC controller. From this figure it is easy to see the effect of J on the closed–loop response, which was explained in section 3.2. Smaller values of J lead to fast responses and aggressive changes in $u(k)$, while larger values of J lead to slower responses and smoother changes in $u(k)$.

Figure 6 shows the responses of the controllers using the control schemes designed above to reject a load disturbance change. The excellent disturbance rejection capabilities of the predictive control algo-

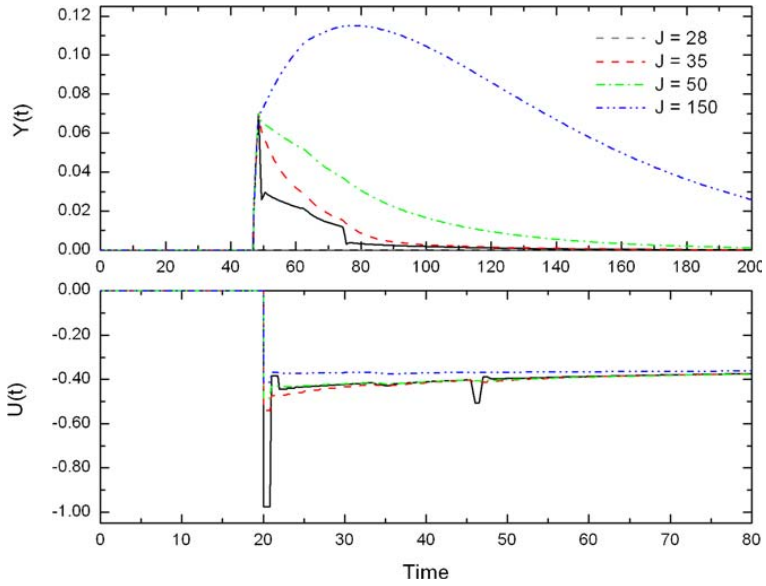

Fig. 5 Closed–loop responses to a step change in disturbance for different values of the prediction time J

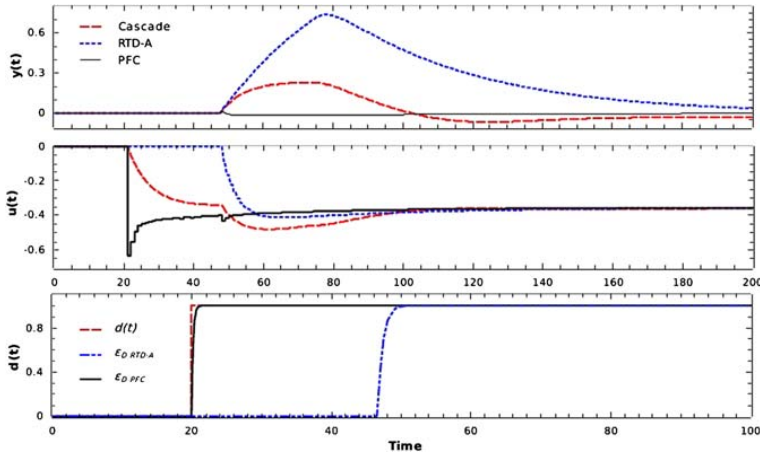

Fig. 6 Closed–loop responses to a step change in disturbance for different control schemes (a) system outputs, (b) manipulated variables, and (c) estimated disturbance for different control schemes

rithms can be clearly seen. The improvement of the closed–loop performance is due to:

(a) a better estimation of the unmeasured disturbance (see Fig. 6(c));
(b) a better model of the effect of the disturbance on the controlled output.

The first two issues are due to the estimation technique employed to built the model used of the PFC controller. Unknown input observers use all available system information to reconstruct the disturbance input. Therefore, no assumption about the disturbance model has being made to built the estimator only model information has been employed. In this way, the model employed to built the PFC controller contains all the available information. Finally, the fact that the PFC controller employs several predicted errors computed in previous samples, introduces a stronger feedback action that improves the closed–loop performance when unmeasured disturbances are presented in the system.

Figure 6(b) shows the control actions employed by each control scheme to reject the disturbance. It is easy to see the feedforward action introduced by the disturbance estimators. The control action is applied to the system as soon as the disturbance is detected in the secondary output. The effect of the difference between the disturbance model employed to built the estimators and the real model can be also seen in this figure. When the effect of the disturbance can be measured in the output y the algorithms correct their predictions, this effect can be also appreciated in the manipulated variable: whereas the PFC controller only corrects the effect of the estimator dynamic (the peak around 50 s), the MPC controller corrects the discrepancy in the disturbance model assumed during the design phase (the peak around 50 s and the subsequent changes until steady state is achieved).

Example 3

This example considers the model of an isothermal polymerization reactor discussed in Maner *et al.* [**37**], where initiator flow rate is used to control the number average molecular weight (NAMW). The non-linear, four-state, state space model (available in the cited reference) is used to represent the true plant. Since, the measurements of NAMW are not available online, the case where an online viscometer provides a surrogate measurement that closely correlates with NAMW with a measurement time delay of 0.1 h is considered.

The non-linear nature of the reactor is shown in Fig. 7, where the NAMW open–loop responses to a sequence of changes in the manipulated variable are shown. This figure shows the dynamic responses to a sequence of changes $+0.1\,m^3/h$, $-0.1\,m^3/h$, $-0.01\,m^3/h$, and $+0.01\,m^3/h$ in the manipulated variable F_{I} about its nominal value $0.017\,m^3/h$. From this figure it is easy to see the non-linear nature of the reactor. The operating space region considered in this example is defined by the hypercube

$$
\begin{aligned}
&|x_1(k)-5.507| \leqslant 5 \text{ kmol}/\text{m}^3\\
&|x_2(k)-0.133| \leqslant 5 \text{ kmol}/\text{m}^3\\
&|x_3(k)-1975| \leqslant 5000 \text{ kmol}/\text{m}^3\\
&|x_4(k)-49.38| \leqslant 5 \text{ kg}/\text{m}^3\\
&|y(k)-25000| \leqslant 15000 \text{ kg}/kmol
\end{aligned}
\tag{36}
$$

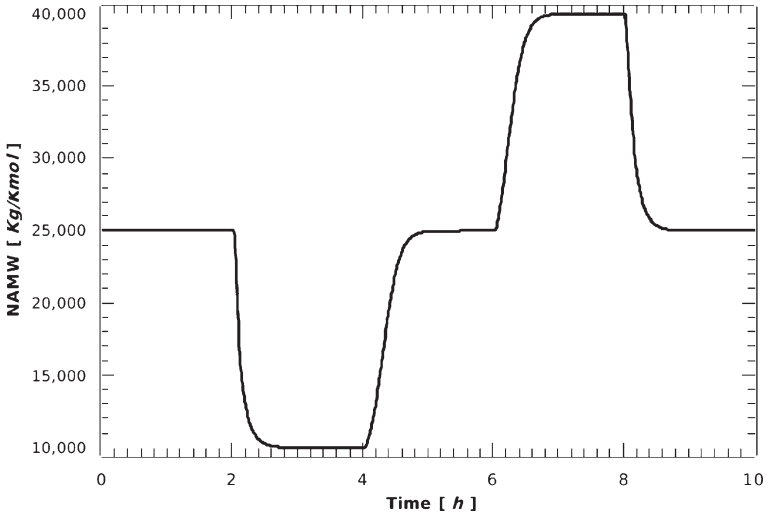

Fig. 7 Open–loop responses of the reactor concentration to step changes in the initiator flowrate $F_I(t)$

Then, it is possible to approximate the non-linear model of the reactor within the specified working space using four linear models, leading to an estimated error $\varepsilon = 0.7$ [**30**]. The linear models were determined from the NAMW step responses and they have been discretized using a zero-order holder in the input and a sampling time of 0.01 h is used. They define the polytopic model $\mathcal{W}$ associated with the non-linear behaviour in the considered operating region.

The controller performance is investigated under a setpoint tracking conditions: beginning from an initial operating steady–state value of 25 000 in NAMW, a sequence of setpoint changes in intervals of 2 h: from 25 000 to 40 000, returns to 25 000, then steps to 10 000 and finally returns to 25 000. The control requirements for this problem are: a zero-offset steady-state response, an overshoot smaller than 5 per cent and a settling time of 1.5 h for an error of 2 per cent.

The performance of the PFC controller is compared with that of an IMC tuned PID [**36**] and RTD-A controller [**15**]. The tuning parameters of the PID and RTD-A controllers are the same as those used in Ogunnaike and Mukati [**15**] (the parameters for the RTD-A controller are: $\theta_R = 0.99$, $\theta_T = 0.1$, $\theta_D = 0.01$, $\theta_A = 0.5$; and the parameters for the IMC-PID controller (with $\lambda = 0.2$) are: $K_C = -7.1759 \times 10^6$, $\tau_I = 0.31$, $\tau_D = 0.0594$).

Model 3 was chosen to represent the reactor because it corresponds to the more sensitive operating region. Design procedure 1 was followed to design the PFC controller in this example. The compensator $F(z)$ was designed using the IMC procedure. Due to the non-linear nature of the reactor, the predictor $P(J, z)$ was built from an estimator, which includes a disturbance observer for the non-measurable disturbance. The disturbance is assumed to enter into the control input ($G_d(z) = G_{p3}(z)$). The parameters chosen for the PFC controller are: $\nu = 1$, $\phi_1 = -1$, $w = 1$, $\theta_0 = 6.1728$, $\theta_1 = -5.8642$ and the prediction times for each model J_l are summarized in Table 1.

While it can be seen from Fig. 8 that the PFC controller provides better setpoint tracking than the RTD-A and PID controllers, the other controllers only outperform it in the first setpoint change. This happens because of the model employed to develop the controllers: while the performance of the RTD-A and PID controllers have been optimized for this change, the PFC was optimized over the entire setpoint trajectory. It is interesting to see that neither the RTD-A nor PID are able to achieve the setpoint in the third change. This fact is due to the change in the process gain (see Table 2). However, in spite of this fact, the PFC achieved the setpoint for all changes due to the adaptation capability introduced by the modification of the prediction horizon J.

Figure 8(b) shows the control action employed by each control scheme to track the setpoint changes. It is easy to see the effect of the adaptation mechanism, which modified the closed-loop behaviour

Table 1 Prediction time for each model of the polytopic model

	Model 1	Model 2	Model 3	Model 4
J	30	45	50	35

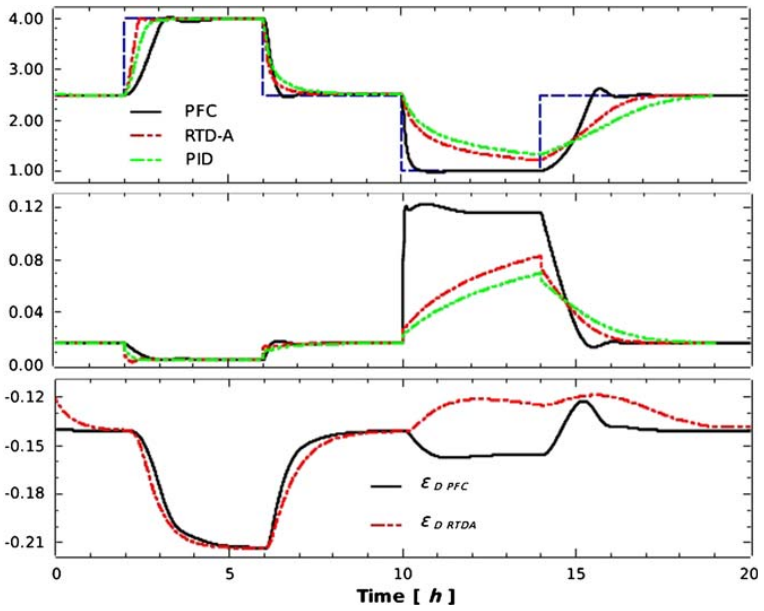

Fig. 8 Closed-loop responses of the reactor to a sequence of step changes in the setpoint for different control schemes (a) system output, (b) manipulated variables, and (c) estimated disturbance for different control schemes

Table 2 Vertices of the polytopic model

Change	Model obtained
Model 1 $F_1 = 0.0170, \quad \Delta F_1 = +0.0999$	$Gp_1(z) = -1.5032 \times 10^5 \dfrac{e^{-0.23}s}{0.115s+1}$
Model 2 $F_1 = 0.0254, \quad \Delta F_1 = -0.0999$	$Gp_2(z) = -1.5032 \times 10^5 \dfrac{e^{-0.42}s}{0.165s+1}$
Model 3 $F_1 = 0.0170, \quad \Delta F_1 = -0.0122$	$Gp_3(z) = -1.2330 \times 10^6 \dfrac{e^{-0.36}s}{0.175s+1}$
Model 4 $F_1 = 0.0086, \quad \Delta F_1 = +0.0122$	$Gp_4(z) = -1.2330 \times 10^6 \dfrac{e^{-0.26}s}{0.115s+1}$

without affecting the system stability. This effect can be clearly seen in the third setpoint change, where the behaviour of the manipulated variable is very different: the PFC quickly follows the change achieving the steady-state value while the others controllers only rely on the integral mode to eliminate the error.

Finally, Fig. 8(c) shows the disturbance estimated by the PFC and RTD-A. In this figure it can be seen that the disturbance observer employed by the PFC tracks the changes in the system faster than the one employed by the RTD-A, providing a better compensation to the unmodelled dynamic and unmeasurable disturbances. It should be noted that for this example both controllers obtain information from the same output, they only differ in the estimation technique employed to reconstruct the unknown input $\tilde{\varepsilon}(k)$.

7 CONCLUSIONS

An alternative method for the design of discrete controllers for SISO systems has been presented and the application and benefits of this strategy has been demonstrated. The PFC controller is a generalization of the IMC structure. It combines the capacity of predictive control algorithms for time-delay com-

pensation, the effectiveness of inferential control schemes for disturbance rejection, and the adaptation capabilities of switching controllers. It is able to maintain consistent setpoint and disturbance rejection performance over the range of non-linear operation.

The contribution of the method presented here include control methodology that:

(a) is straightforward to implement and use;
(b) requires minimal computation;
(c) relies on the linear control knowledge of plant;
(d) is reliable for a broad class of process applications.

Through various simulations the effect of tuning parameters on the controller performance attributes have been shown. The PFC controller was shown to provide a better setpoint tracking and disturbance rejection performance than several controllers, including PID and predictive control algorithms.

ACKNOWLEDGEMENTS

The author wishes to thank: the Agencia Nacional de Promocin Cientfica y Tecnolgica, the Universidad Nacional de Litoral (grants PAE 37122, PAE-PICT-2007-00052), and the Consejo Nacional de Investigaciones Científicas y Técnicas (CONICET), for their support.

REFERENCES

1 **Astrom, K.** and **Hagglund, T.** The future of PID control. *Control Engng Pract.*, 2001, **9**(11), 1163–1175.
2 **Katebi, M.** and **Moradi, M.** Predictive PID controllers. *IEE Proc. Control Theory Appl.*, 2001, **148**(6), 478–487.
3 **Wang, Q., Hang, C.,** and **Yang, X.** Single-loop controller design via IMC principles. *Automatica*, 2001, **37**(12), 2041–2048.
4 **Tan, K., Lee, T., Huang, S.,** and **Leu, F.** PID control design based on a GPC approach. *Ind. Engng Chem. Res.*, 2002, **41**(12), 2013–2022.
5 **O'Dwyer, A.** *Handbook of PI and PID controller tuning rules*, 2003 (Imperial College Press, London).
6 **Lequin, O., Gevers, M., Mossberg, M., Bosmans, E.,** and **Triest, L.** Iterative feedback tuning of PID parameters: comparison with classical tuning rules. *Control Engng Pract.*, 2003, **11**(9), 1023–1033.
7 **Silva, G., Datta, A.,** and **Bhattacharyya, S.** *PID controllers for time delay systems*, 2003 (Birkhäuser, Cambridge, MA).
8 **Haugen, F.** *PID control of dynamic systems*, 2004 (Tapir Forlag, Trondheim, Norway).
9 **Choi, Y.** and **Chung, W.** *PID Trajectory Tracking Control for Mechanical Systems*, 2004 (Springer-Verlag). 2
10 **Johnson, M.** and **Moradi, M.** *PID control: new identification and design methods*, 2005 (Springer Verlag, London).
11 **Astrom, K.** and **Hagglund, T.** *Advanced PID control*, 2005 (ISA, Research Triangle Park, NC).
12 **Wang, Q.-G., Ye, Z., Cai, W.-J.,** and **Hang, C.-C.** *PID Control for multivariable processes*, 2008 (Springer-Verlag). 3
13 **Soroush, M.** and **Muske, K.** Analytical model predictive control. *Prog. Syst. Control Theory*, 2000, **26**(1), 163–179.
14 **Pannocchia, G., Laachi, N.,** and **Rawlings, J.** A candidate to replace PID control: SISO constrained LQ control. *AIChE J.*, 2005, **51**(4), 1171–1189.
15 **Ogunnaike, B.** and **Mukati, K.** An alternative structure for next generation regulatory controllers part I: basic theory for design, development and implementation. *J. Process Control*, 2006, **16**(5), 499–509.
16 **Ergon, R.** On primary output estimation by use of secondary measurements as input signals in system identification. *IEEE Trans. Autom. Control*, 1999, **44**(4), 821–825.
17 **Giovanini, L.** Embedded estimator in predictive feedback control. *ISA Trans.*, 2004, **43**(3), 343–359.
18 **Giovanini, L.** and **Grimble, M.** Generalised predictive feedback control. In Proceedings of the 42nd IEEE Conference on *Decision and control*, 2003, pp. 923–928 (IEEE, Piscataway, NJ). 4
19 **Kitanidis, P.** Unbiased minimum-variance linear state estimation. *Automatica*, 1987, **23**(6), 775–578.
20 **Gillijns, S.** and **de Moor, B.** Unbiased minimum-variance input and state estimation for linear discrete-time stochastic systems. Internal report ESAT-SISTA/TR 05-228, Katholieke Universiteit Leuven, Leuven, Belgium, 2005.
21 **Palanthandalam-Madapusi, H., Gillijns, S., de Moore, B.,** and **Bernstein, D.** System identification for nonlinear model updating. American Control Conference, 2006. 5
22 **Palanthandalam-Madapusi, H.** and **Bernstein, D.** Unbiased minimum-variance filtering for input reconstruction. American Control Conference, 2007.
23 **Keller, J.** Fault isolation filter design for linear stochastic systems. *Automatica*, 1999, **35**(10), 1701–1706.
24 **Morari, M.** and **Zafiriou, E.** *Robust process control*, 1989 (Prentice Hall, Englewood Cliffs, NJ).
25 **Giovanini, L.** Predictive feedback control. *ISA Trans.*, 2003, **42**(2), 207–226.
26 **Keviczky, L.** and **Bányász, C.** Future of the Smith predictor based regulators comparing to Youla 6

parametrisation. In Proceedings of the Mediterranean Conference on *Control and Automation*, 2007, pp. 1–5.

27 **Ydstie, B., Kershenbaum, L.,** and **Sargent, R.** Theory and application of an extended horizon self–tuning controller. *AIChE J.*, 1985, **31**(11), 1771–1780.

28 **Isermann, R.** *Digital control systems*, 1996 (Springer-Verlag, New York).

29 **Arulalan, G.** and **Deshpande, P.** Simplified model predictive control. *Indus. Engng Chem. Res.*, 1987, **26**(2), 347–356.

30 **Angelis, G.** *System analysis, modelling and control with polytopic linear models*. PhD Thesis, University of Eindhoven, 2001.

31 **Mirkin, L.** and **Raskin, N.** Every stabilising dead–time controller has an observer–predictor based structure. *Automatica*, 2003, **39**(10), 1747–1754.

32 **Polyak, B.** and **Shcherbakov, P.** Superstable linear control systems. I. Analysis. *Autom. Remote Control*, 2002, **63**(8), 1239–1254.

33 **Giovanini, L., Benosman, M.,** and **Ordys, A.** Adaptive Control using Multiple Models and Switching. In Proceedings of the IEEE Conference on *Industrial and control applications*, 2005 (IEEE, Piscataway, NJ).

34 **Blanchini, F.** and **Snaizer, M.** A convex optimization approach to fixed–order controller design for disturbance rejection in SISO systems. *IEEE Trans. Autom. Control*, 2000, **45**(5), 784–789.

35 **Prett, D.** and **Morari, M.** The Shell Process Control Workshop,, **47**, 1986, pp. 755–765 (Butterworths, Stoneham, MA).

36 **Ogunnaike, B.** and **Ray, W.** *Process Dynamics, Modelling and Control*, 1994 (Oxford University Press, New York).

37 **Maner, B., Doyle, F., Ogunnaike, B.,** and **Pearson, R.** Nonlinear model predictive control of a simulated multivariable polymerisation reactor using second order Volterra models. *Automatica*, 1996, **32**(9), 1285–1301.

APPENDIX

Notation

$A(z^{-1})$, $B(z^{-1})$, $C(z^{-1})$	system polynomials
$\Delta A(z^{-1})$, $\Delta B(z^{-1})$, $\Delta C(z^{-1})$	parametric uncertainty of the model
$\tilde{A}(z^{-1})$, $\tilde{B}(z^{-1})$, $\tilde{C}(z^{-1})$	model polynomials
$C(z)$	transfer function of the feedback parametrization of the controller
$d(k)$	system measurable disturbance
$\hat{e}^0(k+J, k)$	J-step-ahead conditional predicted error computed at time k
$F(z)$	compensator of the PFC controller
$\tilde{G}p(z)$	system model transfer function
J	prediction horizon
J_l	prediction horizon for the lth model of the polytope $\mathcal{W}$
$J(i)$	prediction horizon at time i
$L(k)$	performance index employed to design the controller
m	number of models belonging to polytope $\mathcal{W}$
M	number of operating regimes of the system
p	order of the model
$Q(z)$	transfer function of the IMC open–loop parametrization of the controller
$P(J, z)$	updated J-step-ahead predictor of system output
$P_l(J_l, z)$	updated J-step-ahead predictor of lth model of the polytopic model $\mathcal{W}$
$\mathcal{P}_y(J, z^{-1})$,$\mathcal{P}_u(J, z^{-1})$ $\mathcal{P}_d(J, z^{-1})$	components of the updated J-step-ahead predictor of system output
$R(z^{-1})$, $W(z^{-1})$	weighting functions of performance index $L(k)$
$\mathcal{S}_{\mathrm{STB}}$	set of prediction times J that lead to stable closed–loop systems
$\Delta_{\mathrm{S}}(z^{-1})$	structural uncertainty of the model
$T(J, z)$	characteristic equation of the closed–loop system for a prediction horizon J
$u(k)$	system input variable
v, w	order of the compensator polynomials
$\mathcal{W}$	polytopic model used to model a system
$y(k)$	system output variable
$\hat{y}(k+J, k)$	J-step-ahead system output prediction
z^{-1}	delay operator
α_j, β_j, γ_j	parameters of the system
$\tilde{\alpha}_j$, $\tilde{\beta}_j$, $\tilde{\gamma}_j$	parameters of the model
$\tilde{\alpha}^l_{jy}$,$\tilde{\beta}^l_{jy}$,$\tilde{\gamma}^l_{jy}$	parameters of the l-step-ahead system output predictor
$\tilde{\alpha}_{j\varepsilon}$, $\tilde{\beta}_{j\varepsilon}$	parameters of the non-measurable disturbance estimator

$\tilde{\alpha}^l_{j\varepsilon}, \tilde{\beta}^l_{j\varepsilon}$	parameters of the l-step-ahead non-measurable disturbance predictor
$\delta(k)$	non-measurable disturbance of the system
ε	approximation error of the polytopic model $\mathcal{W}$
$\varepsilon(k)$	non-measurable disturbance of the model at time k
$\varepsilon_{\mathrm{D}}(k)$	deterministic component of the non-measurable disturbance of the model
$\varepsilon_{\mathrm{S}}(k)$	stochastic component of the non-measurable disturbance of the model
ζ	damping factor of the system
θ_j, ϕ_j	parameters of the compensator polynomials
θ_{A}, θ_{D}, θ_{R}, θ_{T}	parameters of the RTD-A controller
$\Theta(z^{-1})$, $\Phi(z^{-1})$	numerator and denominator of the compensator $F(z)$
κ	tuning parameter of the simplified model predictive controller
μ_{R}, μ_{E}	bound of the reference and error trajectories
τ_{I}, τ_{D}, K_{C}	parameters of the PID controller
ω_{n}	natural frequency of the system